

Journal of Materials Chemistry B

Accepted Manuscript



This is an *Accepted Manuscript*, which has been through the Royal Society of Chemistry peer review process and has been accepted for publication.

Accepted Manuscripts are published online shortly after acceptance, before technical editing, formatting and proof reading. Using this free service, authors can make their results available to the community, in citable form, before we publish the edited article. We will replace this *Accepted Manuscript* with the edited and formatted *Advance Article* as soon as it is available.

You can find more information about *Accepted Manuscripts* in the [Information for Authors](#).

Please note that technical editing may introduce minor changes to the text and/or graphics, which may alter content. The journal's standard [Terms & Conditions](#) and the [Ethical guidelines](#) still apply. In no event shall the Royal Society of Chemistry be held responsible for any errors or omissions in this *Accepted Manuscript* or any consequences arising from the use of any information it contains.

ARTICLE

Viscosity Enhanced Release (VER) Effect in Nanoporous Drug Delivery Systems: Phenomenon and Mechanism

Cite this: DOI: 10.1039/x0xx00000x

Received 00th January 2015,
Accepted 00th January 2015

DOI: 10.1039/x0xx00000x

www.rsc.org/

Di-Wei Zheng,^{a,b} Jiang-Lan Li,^a Cao Li,^b Zu-Shun Xu,^b Si-Xue Cheng^a and Xian-Zheng Zhang^{a,*}

High viscosity is important for normal intracellular homeostasis. In this study, nanoporous drug delivery systems (DDSs) including mesoporous silica nanoparticles (MSNs) and layer by layer (LBL) microcapsules with a viscosity enhanced release (VER) effect were designed and prepared, and their drug release behaviors in a sticky environment with high viscosity were investigated, using Rhodamine B, methylene blue and doxorubicin (DOX) as model drugs. Results showed that the drug release rate from DDSs in biomimetic high viscosity solution was 7-8 times higher than that in water. A semipermeable membrane model was used to explain the VER effect. The result indicated that the existence of macromolecules in release medium caused VER effect. The VER effect found in this study would provide a new concept to guide the design of DDSs in a high viscosity environment in vivo.

Introduction

High viscosity is the nature of living organism. Due to the high concentration of macromolecules such as polysaccharides, lipids, proteins and nucleic acids, the viscosity of intracellular environment is very high. The high-viscosity systems usually have a chaotic and unstable nature,¹ which is trendy to present a dramatic deviation from low-Reynolds-number systems.² Due to the turbulent nature of biofluid,³ it is important to move the research object of the release media for drug delivery systems from classical low-viscosity (LV) simplified systems to high-viscosity (HV) biomimetic systems. However, studies in drug release in micro- and nano-scaled systems in organism with a chaotic nature are very limited.

Developing various drug delivery systems is one of the most exciting research fields in micro- and nanotechnology.⁴⁻⁶ With the help of DDSs, drugs can be delivered to particular sites by active targeting and passive targeting.⁷ However, the drug release behavior was usually studied in low viscosity systems such as water or serum containing media. Since the chaotic and unstable nature of HV systems may create some distinct phenomena which are much different from conventional LV systems. As a result, to study the drug release for in vivo applications, it is essential to use HV release media to mimic

the cellular microenvironment. According to literatures, blood has a viscosity of 4 cp,⁸ cell membrane has a viscosity of 90 cp,⁹ lysosome has a viscosity of 67 cp,¹⁰ cytoplasm has a viscosity of 80 cp and extracellular matrix has a viscosity as high as 540 cp,¹¹ which is about 540 times higher than that of water (1 cp at 20 °C). The high viscosity may suppress the diffusion process of molecules, and affect the release behavior of drug delivery systems.

To our knowledge, the behavior of DDSs in HV solutions has never been studied previously. In this study, the drug release based on mesoporous silica nanoparticles and layer by layer assembly microcapsules were investigated in the release media with different viscosity values. An interesting phenomenon was observed, i.e., the drug release rate from mesoporous silica nanoparticles in a biomimetic HV solution with the same viscosity of lysosome and cytoplasm was 7 times higher than that in a LV solution and the variation trend of the release with the viscosity increased initially and decreased later. Similar finding can also be observed for layer by layer (LBL) microcapsules, which indicated that such a release pattern is common among nano- and micro-carriers. Due to the similarities of DDSs we studied and dialysis bags, a semipermeable membrane model was used to explain the effect

of concentration gradient on the release rate and this viscosity enhanced release effect (VER effect).



Fig. 1 Viscosities of extracellular matrix and different parts of the cell.

Experimental section

Materials

Polyallylamine hydrochloride (PAH, $M_w \sim 15000$) and Rhodamine B were purchased from Sigma Aldrich. Poly(styrenesulfonic acid sodium salt) (PSS, $M_w \sim 70000$) was purchased from J & K Chemical Ltd. Calcium chloride (CaCl_2), potassium carbonate (K_2CO_3), β -cyclodextrin (β -CD), *p*-methyl benzene sulfonic chloride (*p*-TsCl), acetone, methanol, trimethylamine (TEA), dimethyl formamide (DMF), sodium hydroxide (NaOH), hydrochloric acid (HCl), ethylsilicate (TEOS), hexadecyl trimethyl ammonium bromide (CTAB), toluene, ethyl acetate, and hydrofluoric acid were purchased from Shanghai Reagent Chemical Co. (China). Dextran ($M_w \sim 70000$), methacrylic acid (MAA), *p*-aminoazobenzene, acryloyl chloride, azodiisobutyronitrile (AIBN), periodate potassium (KIO_4), ethanediamine (EDA), ethylene diamine tetraacetic acid (EDTA), methylene blue and hydroxy ethyl cellulose (HEC) were purchased from Aladdin Industrial Corporation. Toluene, DMF and MAA were redistilled before used. Doxorubicin (DOX) was purchased from Zhejiang Hisun Pharmaceutical Co. (China). Other reagents were purchased from Shanghai Reagent Chemical Co. (China) and used as received.

Synthesis of mesoporous silica nanoparticles (MSNs)

Mesoporous silica nanoparticles were synthesized according to our previous works.¹² Briefly, 1.0 g of CTAB and 280 mg of NaOH were dissolved in 480 mL DI water and heated to 80 °C. Then 5.0 g of TEOS was added dropwise to the solution under vigorous stirring for about 20 min. The reaction mixture was stirred vigorously at 80 °C for 2 h. The resulting product was centrifuged (10000 r/min, 15 min), washed with water and methanol for three times and dried under vacuum. The obtained MSNs were characterized by transmission electron microscopy (TEM, JEOL-2100, Japan). A mixture of 200 mg of MSNs, 80 mL of methanol and 5 mL of HCl (37.4%) was refluxed at 80 °C for 48 h to remove the CTAB. Then the resulting product

was centrifuged (10000 r/min, 15 min), washed with methanol and water for several times, and then dried with a freeze dryer. After that, 100 mg of MSNs was suspended in a mixture of 5 mL of methanol and 5 mL of DI water. 25 mg of Rhodamine B was added followed by a stirring for 24 h. The product was washed with methanol and water, then lyophilized for 3 days to obtain a white powder. The synthesis of methylene blue and DOX loaded MSNs were prepared with the same way.

Synthesis of dextran-graft- β -CD (Dex-*g*- β -CD)

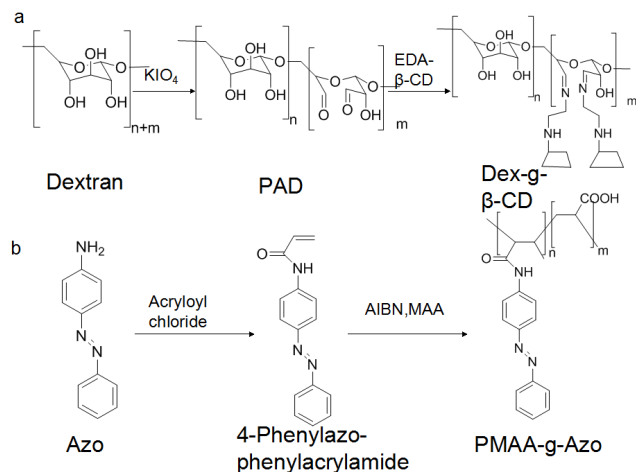
Dex-*g*- β -CD was synthesized according to our previous works.¹³ 10 g of β -CD (8.81 mmol) was dissolved in 300 mL of 0.4 M NaOH solution with a vigorous stirring. Then, 15 g of *p*-TsCl (72 mmol) was added slowly (1 g/min) under ice-bath. After a vigorous stirring for about 1 h under ice-bath, the suspension was filtered. Then HCl was added to the filtrate solution until pH value was adjusted to 5–6. The solution was kept at 4 °C overnight. The precipitate was collected by filtration and washed with acetone for three times. In order to remove unreacted *p*-TsCl and β -CD, the crude product was recrystallized at 80 °C for three times. After being dried at 50 °C for 48 h under vacuum. Then 5.0 g of OTs- β -CD (3.88 mmol) was added in 30 mL of ethylenediamine, the reaction was kept at 80 °C for 12 h. The resultant solution was cooled to room temperature and poured in a large amount of ethanol. The precipitate was dissolved in water/methanol (3:1 v/v). Precipitation and dissolving procedures were repeated twice to wash the product sufficiently. Then, the product was dissolved in water and lyophilized for 3 days. A total weight of 1.00 g of dextran (6.28 mmol of repeat unit) was dissolved in 40 mL of DI water. Then, the solution was protected with N_2 for 30 min. After that, 0.140 g of KIO_4 (0.628 mmol, 10% of dextran repeat unit) was added. The mixture was stirred at 25 °C for 12 h under a N_2 atmosphere. Then, the solution was precipitated by methanol and the white precipitate was collected, followed by 24 h of vacuum drying. After that, 0.5 g of polyaldehyde dextran (PAD) (3.09 mmol of repeat unit) was dissolved in 30 mL of DI water and the solution was purged with N_2 for 30 min. After that, 20 mL of EDA- β -CD (0.544 g, 15% of PAD repeat unit) solution was added. The mixture was stirred at 30 °C for 24 h under a N_2 atmosphere. β -CD was grafted to dextran with the pH-sensitive Schiff's base. Then the product was dialyzed (MWCO: 8000–12000 Da) against DI water for 6 days and then lyophilized for 3 days to obtain the Dex-*g*- β -CD.

Synthesis of azobenzene grafted polymethylacrylic acid (PMAA-*g*-Azo)

4-Phenylazophenylacrylamide was synthesized according to the literature.¹⁴ 1.60 g of 4-aminoazobenzene (8 mmol) and 1.46 mL of triethylamine (10.4 mmol) were dissolved in 40 mL of tetrahydrofuran. 0.8 mL of acryloyl chloride (9.5 mmol) was dissolved in 15 mL of tetrahydrofuran and added dropwise while stirring at 0 °C in a nitrogen atmosphere. Then, the reaction mixture was stirred for 4 h at room temperature. After that, the product was filtered and washed 3 times with water to remove triethylammonium chloride. The product was obtained by evaporating the solvent (1.49 g, 5.93 mmol). Finally, the product was dried under vacuum.

100 mg of AIBN (0.6 mmol), 0.77 g of MMA (7.69 mmol) and 0.56 g of 4-phenylazophenylacrylamide (2.83 mmol) were dissolved in 7.5 mL of DMF. The nitrogen flow was maintained for 20 min before heating. The solution was protected in a N_2 atmosphere with stirring at 65 °C for 24 h. Followed by a

alkaline wash (sodium carbonate, pH=9) and PMAA-g-Azo was dissolved in the NaOH solution with pH value of 9, and then dialyzed (MWCO: 3500 Da) against water with pH of 8 for 6 days. After that, the product was lyophilized for 3 days to obtain orange solid PMAA-g-Azo.



Scheme 1. Synthesis routes of a) Dex-g-β-CD and b) PMAA-g-Azo.

Fabrication of LBL microcapsules

Calcium carbonate microspheres as the template for LBL microcapsules were prepared according to the previous literature.¹⁵ Briefly, 0.228 g of K₂CO₃ and 10 mg of PSS were dissolved in 5 mL of water. Then 0.183 g of CaCl₂ and 5 mg of Rhodamine B were dissolved in 5 mL of water. CaCl₂ solution was added in K₂CO₃ solution under a vigorous stirring for 30 seconds. Then the emulsion was stood for 2 minutes. Calcium carbonate microspheres were collected by centrifuge. The morphology of microspheres was characterized by scanning electron microscope (SEM).

In addition to the electrostatic force, the host-guest interaction between β-CD and azobenzene was also used as a driving force to build the LBL microcapsules. To achieve a positive charge surface, 100 mg of CaCO₃ microspheres were dispersed by 1 mL of PAH polycation solution (1 g/L). Then the suspension was shaken constantly for 15 min to get a PAH layer. After adsorption, the particles were isolated by centrifugation (2500 rpm for 3 min), followed by washing with 2 mL of DI water thrice. Then, 1 mL of PMAA-g-Azo solution was added and shocked for 15 min. The product was centrifuged and washed with DI water thrice. The LBL process was repeated to get PAH(PMAA-g-Azo/Dex-g-β-CD)₁₀ multilayer films. Then 1 mL of 0.4 M EDTA solution with pH 7.4 was added to remove the CaCO₃ core. 2 mL of DI water was used to wash the product. The procedure was repeated for 3 times. After that, microcapsules were centrifuged and washed with DI water thrice and then lyophilized.

Drug loading

LBL microcapsules were damaged by an ultrasonic bath treatment. 10 mg of MSNs was dissolved in 600 μL of HF and then diluted with 2 mL of H₂O. The amount of Rhodamine B was measured with a UV-Vis spectrometer.

Characterizations

Dex-g-β-CD and PMAA-g-Azo were recorded on a Mercury VX-300 spectrometer at 300 MHz NMR (Varian) by using D₂O and DMSO-d₆ as the solvent. Transmission electron microscopy (TEM) images were obtained on a JEM-2100 (JEOL) transmission electron microscope. Scanning electron microscopy (SEM) images were obtained in a JSM6510LV (JEOL) scanning electron microscope. Confocal laser scan microscope (CLSM) images were obtained on a C1-Si (Nikon) confocal laser scan microscope.

Study on the relationship between viscosity and concentration

Hydroxy ethyl cellulose was used as a thickener. Powder of HEC was added into the solution slowly, followed by a vigorous stirring overnight to get solutions with concentrations of 0.1%, 0.2%, 0.4%, 0.5%, 1.0% and 2.0%. A NDJ-9S rotational viscometer was used to measure their viscosity.

In vitro drug release at different viscosity values

3.75 mg of Rhodamine B loaded MSNs or LBL microcapsules were dissolved in 2 mL of solution with a particular viscosity (1 cp, 20 cp, 40 cp, 60 cp and 80 cp) in a dialysis bag (MWCO: 8000-12000 Da). The dialysis bag was immersed into 200 mL of buffer solution to carry out the in vitro drug release study. During the release, 4 mL of solution was withdrawn from the solution periodically. The volume of solution was held constantly by adding 4 mL of buffer solution after each sampling. The concentration of Rhodamine B was measured with a UV-Vis spectrometer (PerkinElmer Lambda Bio 40) by the absorbance at 543 nm.

In vitro simulation by using dialysis bags

1 mL of Rhodamine B solution with a concentration of 1 g/L were put into a dialysis tube (MWCO: 8000-12,000 Da) quickly. Dialysis bags containing 1 mL of Rhodamine B solution (1 mg/mL) were immersed into 40 mL of HEC solutions with viscosities of 1 cp, 20 cp and 540 cp, respectively. After 1 min of co-incubation, the concentration of Rhodamine B out of the dialysis bag was measured with a UV-Vis spectrometer.

Results and discussion

Characterization of Dex-g-β-CD and PMAA-g-Azo

Dex-g-β-CD was synthesized from PAD and EDA-β-CD. As shown in the ¹H NMR spectra (Fig. 2), for EDA-β-CD, peaks around δ 2 to δ 3 were due to the alkyl chain of ethanediamine. Attribution of hydrogen atoms for cyclodextrin was shown in the Fig. 2a. For Dex-g-β-CD, peaks appeared at δ 4.9 and δ 2.4. Peaks appeared at δ 2.6 and δ 3.1 were attributed to protons of positions 4 and 1 of EDA-β-CD. The peak at δ 4.8 was due to protons of positions 1 which were contributed to an anomeric carbon atom. There is no peak in δ 5.0 to 5.7, indicating that aldehyde groups of PAD were fully replaced by EDA-β-CD. Three groups of peaks between δ 4.0 and δ 3.2 were attributed to the proton in positions C2-C6 of dextran.¹⁶

For PMAA-g-Azo shown in Fig. 2b, peaks around δ 1 were attributed to methyl groups of PMAA. Peaks around δ 2 were due to the alkyl chain of PMAA. Small peaks around δ 7.0~ 8.0 were contributed to the azobenzene.

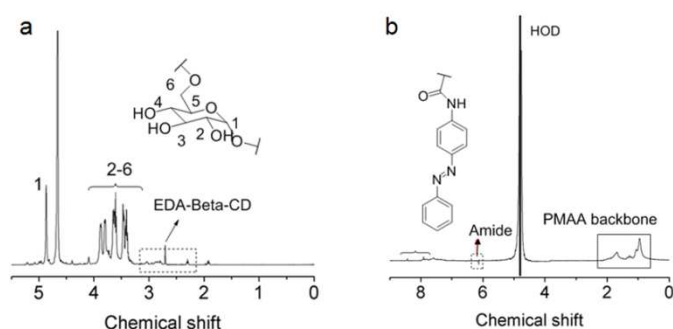


Fig. 2 a) $^1\text{H-NMR}$ spectra of a) Dex- g - β -CD, and b) PMAA- g -Azo.

Characterizations of MSNs and LBL capsules

In this study, CaCO_3 microspheres as the template for LBL capsules exhibited a regular spherical shape in the SEM image (Fig. 3a). As shown in Fig. 3b, the collapsed LBL microcapsules were observed by TEM exhibited a clear layer structure. Bright red dots were observed with a confocal fluorescent microscopy in Fig. 3d. The diameter of about 1–2 μm was much closed to CaCO_3 microspheres. Shown in Fig. 3c, Red fluorescent dots excited from Rh B with a wavelength of 543 nm laser showed that Rh B was captured between capsule walls. The result indicated that microcapsules were prepared successfully. Mono-dispersed mesopore MSNs with a regular spherical shape and an average diameter of 130 nm can be observed (Fig. 3d). The clear mesoporous structure with an average pore size of about 1–2 nm indicated that CTAB was fully removed.

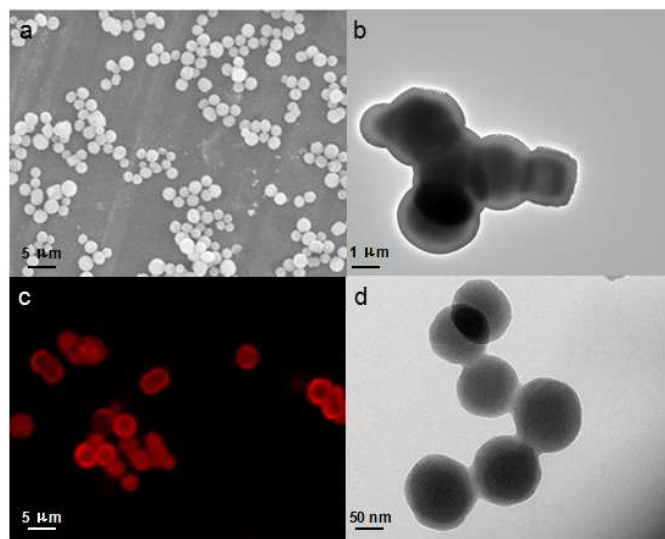


Fig. 3 Images of microcapsules and mesopore silica nanoparticles. a) SEM image of CaCO_3 template. b) TEM image of microcapsules. c) Confocal microscope image of microcapsules. d) TEM image of mesopore silica nanoparticles.

Viscosity-concentration fit curve of HEC solution

A rotational viscometer was employed to measure the concentration of HEC solutions at 20 $^\circ\text{C}$. It can be observed that

dates plotted for varying viscosity resulted in a universal quadratic curve (Fig. 4a). A significant quadratic relation was found between viscosity and concentration. With the increase in concentration, the derivative constantly increased, which was due to the polymer chain overlap with each other and the hydrodynamic interactions between these polymer coils.^{17,18}

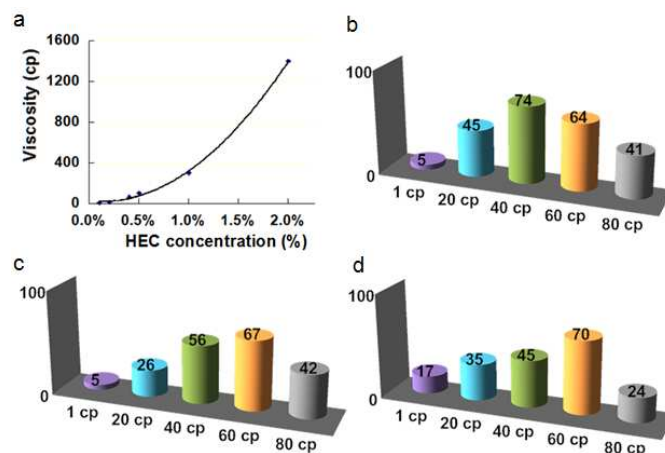


Fig. 4 a) Viscosity-concentration curve of HEC. Cumulative drug release in 5 h of MSNs in the solutions with different viscosities by using the model drug of b) Rh B, c) methylene blue or d) DOX.

In vitro drug release under different viscosities

It is a universal acknowledgment that the increase of viscosity will suppress the diffusion process and reduce the drug release rate significantly. However, our study suggested that instead of inhibiting release rate, the HV environment enhanced the release of Rh B. As shown in Fig. 4b, for 40 cp group, 75% of drug was released in 6 h, which was approximately 7 times faster compared to 5% drug release at 1 cp group. However, an ultra-high viscosity can suppress the diffusion process. These two factors affect the drug release behavior of DDSs simultaneously. Under the viscosity of 40 cp, which was closed to the intracellular viscosity *in vivo*, the speed of release achieved its maximum value. Methylene blue, a widely used photodynamic therapy drug and the anti-cancer chemotherapy drug DOX were also used as model drugs, the same finding was observed as shown in Fig. 4c and d. However, this phenomenon provided a potential passive targeting for intracellular delivery since MSNs have an accelerated drug release in the environment with a viscosity similar to intracellular micro-environment.

In order to further study this novel phenomenon, the effect of viscosity on the release rate from LBL microcapsules were also investigated. As depicted in Fig. 5a, for LBL microcapsules, the same phenomenon was also observed. The release rate under 40 cp was 8 times higher compared to the control group under 1 cp. The maximum release rate also appeared at around 40 cp and this coincidence indicated that the VER effect of both MSNs and LBL microcapsules may be a result of the similarity related to their nanoporous structures with permselectivity.

To our knowledge, LBL microcapsules have a similarity with the semipermeable membrane.¹⁹ This characteristic has been used to design “active defense” LBL microcapsules, which were studied in our previous work.²⁰ MSNs have mesopores with a diameter about 1–2 nm which was very close to dialysis bag with a MWCO of 1–30 kDa.²¹ And for mesopores zeolite

crystals systems, Hayhurst and Wernickif developed the theory of membrane permeation to explain the diffusion procedure in zeolite molecular sieves.^{22,23} Due to the similarity between zeolite and MSNs or LBL microcapsules, the theory of membrane permeation can also be applied to MSNs and LBL microcapsules to explain the VER effect. MSNs have some feature of semipermeability with the existence of the nanoporous structure, which exhibited a similarity with functional semipermeable membrane.²⁴ Nanopores in both MSNs and LBL capsules made small solutes readily permeate through the matrices. In contrast, higher molecular weight solutes diffused restrictily into the matrices due to the small size of the nanopores. Since HEC chains have a steric hindrance effect, it is impossible for them to diffuse through the membrane. A concentration gradient between inner and outer of carriers was created. This concentration gradient led to a great osmotic pressure and forced loaded molecules diffused out from DDSs to the solution. However, when the viscosity of the solution was high enough to inhibit the diffusion process, the release rate could not further increase. As a result, the rising of concentration inhibited the release rate of drug and caused a higher cumulative drug release.^{25,26}

The diffusion process of loaded molecules from DDSs can be described by the Solution-Diffusion Model²⁷ with the perfect membrane:

$$J_w = A(\Delta P - \Delta \pi) \quad (1)$$

where J is the permeate flow of small molecules such as model drugs or water, A is the small molecules permeability coefficient, ΔP is the applied pressure driving force (a function of the feed, concentration and permeate pressures) and for the DDS, $\Delta P = 0$, $\Delta \pi$ is the osmotic pressure of the solution.

By using Van 't Hoff equation of osmotic pressure:

$$\pi = C_B RT \quad (2)$$

where π is the osmotic pressure, concentrations of drug molecules on both sides of the semipermeable membrane are equal and C_B is the concentration of molecules that can hardly pass through the semipermeable membrane and for drug delivery systems approximately.

$$C_B = C_{ECM} \quad (3)$$

High viscosity can suppress the penetration process²⁸

$$J_w = \alpha L^{water} \frac{\Delta P}{\mu_B}$$

where J is the permeate flow of small molecules, α is an empirical parameter, ΔP is the applied pressure driving force, μ_B is the viscosity of the solution and L^{water} is the intrinsic membrane water permeability. For a steady state process, ΔP can be considered as zero approximately.²⁹

Since the molecules permeability coefficient is inversely proportional to the solution viscosity

$$J_w = K \times \frac{C_B}{\mu_B} \quad (4)$$

where K is a constant, C_B is the concentration of HEC molecule and μ_B is the viscosity of the solution.

With the Huggins equation form viscosity-concentration function³⁰, viscosity (μ_B) can be expressed in terms of a single variable with concentration as follows:

$$\mu_B = 3.9 \times 10^6 C_B^2 - 8692.2 C_B + 22.037 \quad (5)$$

in which μ_B is the viscosity of the HEC solution and c is the concentration of the HEC solution.

As a result, the permeate flow- concentration relationship can be expressed as

$$J_w = K \times \frac{C_B}{3.9 \times 10^6 C_B^2 - 8692.2 C_B + 22.037} \quad (6)$$

By taking a derivative with respect to concentrations, a maximum value was found with a concentration of 0.24%. The corresponding viscosity of this point was about 23 cp. This result was in a very accordance with our experiment result. These theoretical calculations proved that the VER effect was attributed to the selective permeable feature of DDSs and physical properties of polymer dilute solution. The theoretical calculated results were in good agreement with our experimental observations.

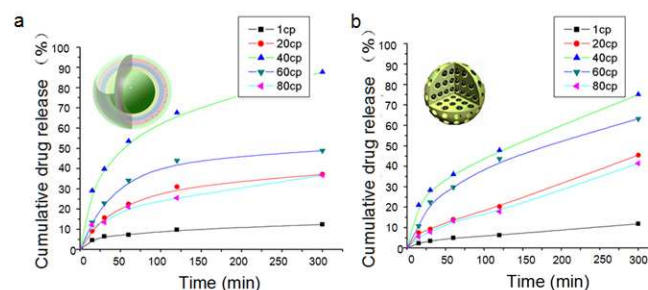


Fig. 5 Drug release curves of a) LBL microcapsules loaded with Rh B, b) MSNs loaded with Rh B.

Macroscopic simulation

With the dialysis bag model, the VER effect was explained qualitatively. After co-incubation for 1 min, the concentration of 1 cp group was 7.51×10^{-7} mol/L and the 20 cp group was 9.7×10^{-7} mol/L, which was 30% higher than the LV group. The result was similar to the previous VER effect in microscale. This macroscopic phenomenon was mainly due to the higher concentration of 20 cp group, which led to a higher osmotic pressure. As a result, Rb molecules diffused through the dialysis membrane with a mesostructure. However, when the viscosity reached to 540 cp which was very similar to the viscosity of extracellular matrix, the high viscosity suppressed the diffusion process effectively. For 540 cp group, a

concentration of 3.8×10^{-7} mol/L was measured which was approximately 2 times higher compared to the 1 cp group.

As detailed above, the VER effect observed in the experiments can be well explained by the theoretical analysis. The macroscopic dialysis bags experiment provided a qualitative tendency which fitted the VER effect curve that initially increased and then gradually declined. This result indicated a high probability that the increase of concentration gradient controlled the release rate of DDSs with a selective permeable feature. However, when the viscosity was high, the process of diffusion was suppressed. The competition between these two factors resulted in the highest drug release rate in a viscosity close to intracellular environment.

However, since the intracellular viscosity is mainly due to the high concentration of macromolecules such as polysaccharides, lipids, proteins and nucleic acids.³¹ The concentration of these biomacromolecules in cells is about 300–400 g/L.³² Consequently, the VER effect can be adapt to the real micro-environment in intracellular level. In addition, the VER effect provides a strategy for intracellular targeting drug delivery to minimize the drug leakage during blood circulation and to avoid serious side effects.³³ These systems could encapsulate the drug in the blood whereas allow the explosive drug release after enter into cells once accumulating in the tumor site. Since the blood viscosity value around solid tumor is 2 times higher than that in normal blood vessel with same red blood cell hematocrit.³⁴ As a result, the VER effect is also a potential exploitation for the treatment of cancer. Compared with other targeting strategy, the simplicity and high efficiency of VER effect may provide a great potential for clinic applications.

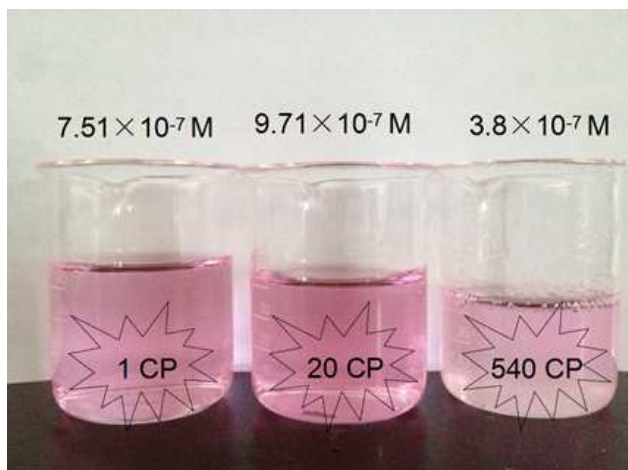


Fig. 6 Rb release from dialysis bags immersed in the media with different viscosities: 1 cp, 20 cp and 540 cp. Rb concentrations out of the dialysis bags were 7.51×10^{-7} mol/L, 9.7×10^{-7} mol/L and 3.8×10^{-7} mol/L, respectively.

Conclusions

In summary, we have demonstrated a novel VER effect with both experimental test and theoretical analysis. The highest release rate from MSNs and LBL microcapsules was found to be achieved in the release medium with a viscosity of 40 cp, which is similar to the lysosome and cytoplasm. On the basis of the molecular diffusion equation, Fick's first law of diffusion and Huggins equation, a mathematical model was established. These results were consistent with the fact that reasonable high viscosity of solution produced faster drug release at a

microenvironment with the viscosity similar to the intercellular microenvironment for drug delivery system like MSNs and microcapsules. The VER effect is of importance for DDSs design. The DDSs developed based on the VER effect may have a great potential in clinical applications.

Acknowledgements

This work was supported by the Ministry of Science and Technology of China (2011CB606202), the National Natural Science Foundation of China (21474077), the Ministry of Education of China (20120141130003) and the Fundamental Research Funds for the Central Universities.

Notes and references

- 1 B. J. Nelson and K. E. Peyer, *ACS Nano*, 2014, 8, 8718–8724.
- 2 H. C. Berg and L. Turner, *Nature*, 1979, 278, 349–351.
- 3 J. B. Grotberg and O. E. Jensen, *Annu. Rev. Fluid Mech.*, 2004, 36, 121–147.
- 4 J. Zhang, Z. F. Yuan, Y. Wang, W. H. Chen, G. F. Luo, S. X. Cheng, R. X. Zhuo and X. Z. Zhang, *J. Am. Chem. Soc.*, 2013, 135, 5068–5073.
- 5 Y. H. Roh, J. B. Lee, K. E. Shopsowitz, E. C. Dreaden, S. W. Morton, Z. Y. Poon, J. K. Hong, I. Yamin, D. K. Bonner and P. T. Hammond, *ACS Nano*, 2014, 8, 9767–9780.
- 6 J. E. Chung, S. Tan, S. J. Gao, N. Yongvongsoontorn, S. H. Kim, J. H. Lee, H. S. Choi, H. Yano, L. Zhuo, M. Kurisawa and J. Y. Ying, *Nat. Nanotechnol.*, 2014, 9, 907–912.
- 7 T. M. Allen and P. R. Cullis, *Science*, 2004, 303, 1818–1822.
- 8 D. Wirtz, K. Konstantopoulos and P. C. Searson, *Nat. Rev. Cancer.*, 2011, 11, 512–522.
- 9 L. Wang, Y. Xiao, W. Tian and L. Z. Deng, *J. Am. Chem. Soc.*, 2013, 135, 2903–2906.
- 10 M. K. Kuimova, G. Yahsioglu, J. A. Levitt and K. Suhling, *J. Am. Chem. Soc.*, 2008, 130, 6672–6673.
- 11 G. M. Lee, F. Zhang, A. Ishihara, C. L. McNeil and K. A. Jacobson, *J. Cell. Biol.*, 1993, 120, 25–33.
- 12 D. Xiao, H. Z. Jia, J. Zhang, C. W. Liu, R. X. Zhuo and X. Z. Zhang, *Small*, 2014, 10, 591–598.
- 13 C. Li, G. F. Luo, H. Y. Wang, J. Zhang, Y. H. Gong, S. X. Cheng, R. X. Zhuo and X. Z. Zhang, *J. Phys. Chem. C.*, 2011, 115, 17651–17659.
- 14 M. G. Rodríguez, mL Tejedaa, JEscalanteb, JA Guerrero-Álvarezb and ME Nicho, *Mater. Chem. Phys.*, 2010, 124, 389–394.
- 15 G. B. Sukhorukov, D. V. Volodkin, A. M. Günther, A. I. Petrov, D. V. Shenoy and H. Möhwald, *J. Mater. Chem.*, 2004, 14, 2073–2081.
- 16 D. Usov and G. B. Sukhorukov, *Langmuir*, 2010, 26, 12575–12584.
- 17 B. Stadler, D. P. Andrew, R. Chandrawati, L. H. Rigau, A. N. Zelikin and F. Caruso, *Nanoscale*, 2009, 1, 68–73.
- 18 P. Gupta, C. Elkinsb, T. E. Longb and G. L. Wilkes, *Polymer*, 2005, 4799–4810.
- 19 J. Roovers, *Macromolecules*, 1994, 27, 5359–5364.
- 20 J. Zhang, X. D. Xu, Y. Liu, C. W. Liu, X. H. Chen, C. Li, R. X. Zhuo and X. Z. Zhang, *Adv. Funct. Mater.*, 2012, 22, 1704–1710.
- 21 X. S. Peng, J. Jin and I. Ichinose, *Adv. Funct. Mater.*, 2007, 17, 1849–1855.
- 22 A. Paravar, D. T. Hayhurst, *In Proceedings of the 6th international zeolite conference*, Olson D and Bisio A ed., Reno, Butterworths, Guildford, UK, 1983, p 217.
- 23 D. L. Wernick, E. J. Osterhuber, *In Proceedings of the 6th international zeolite conference*, D Olson and A Bisi ed., Reno, Butterworths, Guildford, UK, 1983, p 122.
- 24 J. Yina, E. S. Kima, J. Yang and B. L. Deng, *J. Membrane. Sci.*, 2012, 423, 238–246.
- 25 C. R. Wilke and P. Chang, *AIChE. J.*, 1955, 1, 264–270.
- 26 R. J. Ellis, *Curr. Opin. Struc. Biol.*, 2001, 11, 114–119.
- 27 M. A. Chaudry, *J. Membrane. Sci.*, 2002, 206, 319–332

ARTICLE

- 28 D. R. Machado, D. Hasson and R. Semiat, *J. Membrane. Sci.*, 2000, 14, 63-69.
- 29 A. E. Velasco, S. G. Friedman, M. Pevarnik, Z. S. Siwy, and P. Taborek, *Phys. Rev. E.*, 2012, 86, 025302.
- 30 J. Desbrieres, *Biomacromolecules*, 2002, 3, 342-349.
- 31 S. B. Zimmerman and S. O. Trach, *J. Mol. Biol.*, 1991, 222, 599-620.
- 32 L. Zhao, Y. H. Xu, T. Akasaka, Si. Abe, N. Komatsu, F. Watari and X. Chen, *Biomaterials*, 2014, 35, 5393-5406.
- 33 W. G. Ashley, J. Henise, R. Reid and D. V. Santi, *Proc. Natl. Acad. Sci. USA.*, 2013, 110, 2318-2323.
- 34 E. M. Sevick, R. K. Jain, *Cancer. Res.*, 1989, 49, 3513-3519.

Notes and references

^a Key Laboratory of Biomedical Polymers of Ministry of Education & Department of Chemistry, Wuhan University, Wuhan 430072, P. R. China. E-mail: xz-zhang@whu.edu.cn

^b Hubei Collaborative Innovation Center for Advanced Organic Chemical Materials; Key Laboratory for the Green Preparation and Application of Functional Materials of Ministry of Education, Hubei University, Wuhan, Hubei 430062, P. R. China

Graphic Abstract

Viscosity Enhanced Release (VER) Effect in Nanoporous Drug Delivery Systems: Phenomenon and Mechanism

Di-Wei Zheng, Jiang-Lan Li, Cao Li, Zu-Shun Xu, Si-Xue Cheng and Xian-Zheng Zhang

Nanoporous drug delivery systems (DDSs) including mesoporous silica nanoparticles (MSNs) and layer by layer (LBL) microcapsules with a viscosity enhanced release effect (VER effect) were demonstrated, and their drug release behaviors in a sticky environment with high viscosity were investigated.

